AGU ADVANCING EARTH AND SPACE SCIENCE

Geophysical Research Letters

RESEARCH LETTER
10.1029/2021GL093670

Key Points:

- The synoptic patterns associated with the summer regional extreme precipitation events over East China during 1961–2018 have been identified
- Cause of the changes of summer regional extreme precipitation over each subregion of eastern China have been discussed.

Supporting Information:

Supporting Information may be found in the online version of this article.

Correspondence to:

A. Huang,
anhuang@nju.edu.cn

Citation:

Tang, Y., Huang, A., Wu, P., Huang, D., Xue, D., & Wu, Y. (2021). Drivers of summer extreme precipitation events over East China. *Geophysical Research Letters*, *48*, e2021GL093670. https://doi.org/10.1029/2021GL093670

Received 5 APR 2021
Accepted 21 MAY 2021

Drivers of Summer Extreme Precipitation Events Over East China

Yong Tang[1], Anning Huang[1,2], Peili Wu[3], Danqing Huang[1], Daokai Xue[1], and Yang Wu[1]

[1]CMA-NJU Joint Laboratory for Climate Prediction Studies, School of Atmospheric Sciences, Nanjing University, Nanjing, China, [2]State Key Laboratory of Severe Weather and Joint Center for Atmospheric Radar Research of CMA/NJU, School of Atmospheric Sciences, Nanjing University, Nanjing, China, [3]Met Office Hadley Centre, Exeter, UK

Abstract Extreme summer precipitation often associated with flash floods has devastating impact on the local economies and livelihood of millions of people over East China. Tracking down the drivers of those extreme events will help to understand their formation mechanisms and to improve forecasts. Here the synoptic patterns associated with summer extreme precipitation events over East China during 1961–2018 have been identified systematically and quantitatively using a circulation clustering method. The results show that regional events over East China are dominated by the Eastern Asian summer monsoon associated Meiyu front, landfalling tropical cyclones and low-pressure vortices. Most sub-regions have seen increasing trends of extreme rainfall events during the past 6 decades with comparable contributions from the two main drivers. There was a decreasing trend over the North China Plain driven by the low-level southeasterly winds.

Plain Language Summary Closely linked to flash floods, extreme precipitation is one of the high impacts but low probability weather phenomena that challenge modern numerical predictions. However, models are generally more skillful in predicting synoptic weather systems than precipitation itself. Taking East China as an example, this paper demonstrates the links between extreme precipitation events and synoptic weather systems using circulation clustering. Two major weather systems, the Eastern Asian Summer Monsoon and landfalling tropical cyclones are responsible for most extreme precipitation events (about 70%) over East China during the summer season. If models can accurately predict the strength and position of these weather systems, there may be enhanced potential of predicting regional precipitation extremes. Such implications are not regionally limited.

1. Introduction

Extreme precipitation (EP) is responsible for floods (van Oldenborgh et al., 2017) and causes widespread destruction of infrastructures, economic damages, and the loss of lives(Keller & Atzl, 2014; Rosenberg et al., 2010; Rosenzweig et al., 2002; Vogel et al., 2019). An increasing body of observational evidence has shown consistent intensification of precipitation extremes from different parts of the planet (Donat et al., 2016). Observations show that maximum hourly summer rainfall intensity has increased by about 11.2% on average in China, and the corresponding event accumulated precipitation has increased by more than 10% on average (Xiao et al., 2016). Global warming is projected to drive further intensification of precipitation extremes toward the future due to increased moisture supply in the atmosphere (Beniston et al., 2007; H. Chen, 2013; Kharin et al., 2013; Tebaldi et al., 2006). Climate prediction and risk assessment of future precipitation extremes have vital importance for impact management and climate change adaptation.

However, limited by insufficient observations and model resolution, it remains a great challenge to adequately describe, simulate, and predict the process of precipitation and precipitation extremes (Pfahl et al., 2017; Q. Zhang et al., 2017). It is very much desirable to explore alternative novel methods to best utilize current model predictions and climate projections for impact assessment and adaptation planning. One of such methods is to identify the synoptic weather patterns leading to EP (Utsumi et al., 2016, 2017).

It is known that EP over East China has the largest amount in summer (Yao et al., 2010) and can be caused by the synoptic systems such as the Meiyu front, tropical cyclone (TC), and low vortex (R. C. Y. Li & Zhou, 2015; Luo et al., 2016; Wu et al., 2016; Xie et al., 2018; C. Zhang et al., 2008; Q. Zhang et al., 2017). The

middle- and upper-level atmospheric circulation systems also play important roles in the formation of EP, that is, the location of western North Pacific subtropical high (WNPSH), the strength of South Asian High (SAH), as well as the location of upper-level Eastern Asian Subtropical Jet (EASJ), all significantly affect the EP over East China(Ge et al., 2019; Huang et al., 2014; L. Li & Zhang, 2014; Ning et al., 2017; Yokoyama et al., 2017; Q. Zhang et al., 2017). And the configuration of these systems, such as the combined effect of WNPSH and SAH, can lead to persistent EP events (Y. Chen & Zhai, 2014). Thus, different configurations of these weather systems can form various synoptic patterns and further result in the regional extreme precipitation events (REPE) with distinct characteristics.

Some earlier studies have been conducted to reveal the synoptic patterns through cluster analysis, such as k-means (Amini & Straus, 2019; Fereday et al., 2008; Riddle et al., 2013; Stahl et al., 2006), self-organizing maps (SOM) (Horton et al., 2015; Ohba & Sugimoto, 2019; Schlef et al., 2019), and hierarchical clustering(Hu et al., 2019; Wu et al., 2016). And the synoptic patterns associated with REPE have been revealed over some regions via clustering method (Houssos et al., 2008; Swales et al., 2016). Most studies perform clustering on single-level fields such as 500 hPa geopotential height, sea level pressure or upper-level zonal wind, which may be not convincing enough to reveal the synoptic patterns related to REPE that is the result of combination effect of multi-level circulation systems. Moreover, the coverage of the input fields in these studies are too large, which is not conducive to reveal the regional circulation characteristics. Here, clustering is applied on wind fields at the lower to upper troposphere within each sub-region of East China to identify the synoptic patterns associated with the REPE.

Here, we aim to answer the following two questions: (1) what are the synoptic patterns responsible for the REPE over each sub-region of East China in summer? (2) what are the temporal variations of these patterns during 1961–2018?

2. Data and Methods

2.1. Rain Gauge Data and Reanalysis Data

Twelve-hourly (20:00–08:00 and 08:00–20:00 Beijing time) rain gauge data are obtained from the Chinese Meteorological Administration (CMA), which covers 2,424 weather stations for June, July, and August during 1961–2018. Six-hourly geopotential height, wind and vertical velocity data with a resolution of 2.5° in latitude by 2.5° longitude are downloaded from the National Centers for Environmental Prediction/National Center for Atmospheric Research (NCEP/NCAR) reanalysis at https://psl.noaa.gov/data/gridded/data.ncep.reanalysis.pressure.html. The NCEP/NCAR dataset is then projected to the same 12-hourly interval consistent with the gauge data. The best-track dataset of TCs from CMA (Ying et al., 2014) is used to verify the contribution of TCs and available at http://tcdata.typhoon.org.cn/. The ERA5 dataset with a 0.25° × 0.25° horizontal resolution during 1979–2018 (https://www.ecmwf.int/en/forecasts/datasets/reanalysis-datasets/era5) is also used for comparison.

2.2. Definition of Extreme Precipitation and Regional Events

Based on the 12-hourly rainfall amount data during summers of 1961–2018, an EP event is defined as where the accumulated 12-hourly precipitation exceeds the 95th percentile threshold of all historical rainfall records that exceeds 0.1 mm at a given location. Following Xie et al. (2018), number of stations with EP events is counted at all 12-h during summers of 1961–2018 over a sub-region, then the REPE are defined when the number of stations with concurrent EP events exceeds the 95th percentile of these counted station numbers (minimum 1).

2.3. Definition of SAH, WNPSH, and EASJ

The SAH is shown by the 12,500 gpm contour at 200 hPa (Ning et al., 2017) and the WNPSH is indicated by the 5,880 gpm contour at 500 hPa. The axis of upper-level EASJ is determined by the composite location of jet core defined as latitude with the maximal zonal wind within 25°–55°N along each longitude between 70° and 150°E at 200 hPa (Yokoyama et al., 2017).

2.4. Clustering Method

Spectral clustering is a modern clustering algorithm that outperforms traditional clustering algorithms such as k-means in many cases (von Luxburg, 2007), it performs traditional clustering on affinity matrix rather than raw data and is rarely applied in the atmospheric science yet.

Python machine learning package (Pedregosa et al., 2011) containing spectral clustering is used to conduct cluster analysis on the wind fields at 925, 850, 700, 500, and 200 hPa during REPE. Each record of u or v at a grid point is regarded as a feature, and the wind fields are two three-dimensional arrays (u and v) during a regional event, they are flattened (axis by axis) to one-dimensional arrays and merged together (v follows u) to form a sample, the order of features will not influence the results of clustering, just make sure to use the same rule to flatten the arrays of all events. Finally, a matrix with shape of n_samples × n_features is obtained as the input data in each sub-region (n_samples refers to the number of samples, it is the total cases of REPE over a given sub-region here, and n_features refers to the number of features), and standardization of the matrix should be done along the sample axis before the input. Some options in the algorithm need to be set, that is, the "nearest_neighbors" is set to construct the affinity matrix and the "kmeans" is selected to assign the cluster labels.

3. Results

3.1. Background

Based on the 12-hourly rainfall amount data, EP is detected at 2,424 stations over China. Figure 1 shows the observational characteristics of summer EP in China for the period of 1961–2018, including the distributions of weather stations and sub-regions (Figure 1a), EP frequency (Figure 1b), EP amount (Figure 1c), and the historical trends of EP frequency (Figure 1d). High frequency occurs in southwestern China and southeastern Tibetan Plateau while high amount spreads from western Sichuan Basin to the southern coast. Significant increasing (decreasing) trends of EP frequency mainly concentrate in the Lower reach of the Yangtze River Basin (North China and Sichuan Basin), which is consistent with previous studies (Dong et al., 2011; Su et al., 2006; Wang & Zhou, 2005; H. Zhang & Zhai, 2011). Trends of EP amount show similar distribution as the frequency (not shown).

According to above backgrounds, East China is divided into four sub-regions: southeastern China, the Lower reach of the Yangtze River basin, North China Plain, and northeastern China, the REPE thresholds are 34, 33, 39, 19 stations, the total stations are 405, 370, 467, 181, and the total occurrences of REPE are 413, 330, 309, 299, respectively. For each sub-region, records at grids within the green box shown in Figure 1 and surrounding grids within 1° are used for clustering (grids used for the four sub-regions are 42, 20, 20, 36, respectively).

3.2. Synoptic Patterns Responsible for Regional Extreme Precipitation Events

Cluster analysis identifies three synoptic patterns over southeastern China, the Lower reach of the Yangtze River Basin, northeastern China and two patterns over North China Plain (Figure 2) (cluster number is an input parameter and determined by objective score [Caliński & Harabasz, 1974], details are shown in the Supporting Information). The occurrence probability of EP at a station is defined as the ratio of total EP occurrences under a given synoptic pattern to the total occurrences of the specific synoptic pattern. Higher occurrence probability implies that the EP is more likely to happen there under such pattern. Over southeastern China, the monsoon-like synoptic pattern 1 characterized by low-level prevailing southwesterly contributes about 72% of total REPE, with higher EP occurrence probability concentrated in the north inland area (Figure 2a). Patterns 2 and 3 are cyclone-like patterns (Figures 2b and 2c), and most cases of pattern 2 (3) are consist of landfalling TCs moving northward (northwestward) (Figures 3a and 3b). High EP occurrence probability (more than 24%) concentrates along the coastal areas under these two patterns. Over the Lower reach of the Yangtze River Basin, the monsoon-like synoptic pattern 1 leads to around 57% of total REPE, with higher EP occurrence probability spreading along the Yangtze River (Figure 2d). Low-level winds under the monsoon-like pattern 2 have typical characteristics of the Meiyu front with easterly (southwesterly) located in the north (south) (Zheng et al., 2008), and EP is more likely to occur in the south (Figure 2e). More than 90% cases of the cyclone-like pattern 3 are resulted from the landfalling TCs (Figure 3c) and EP tends to happen along the eastern coast (Figure 2f). Over northeastern China, the cyclone-like pattern 1 is characterized by a low vortex and contributes

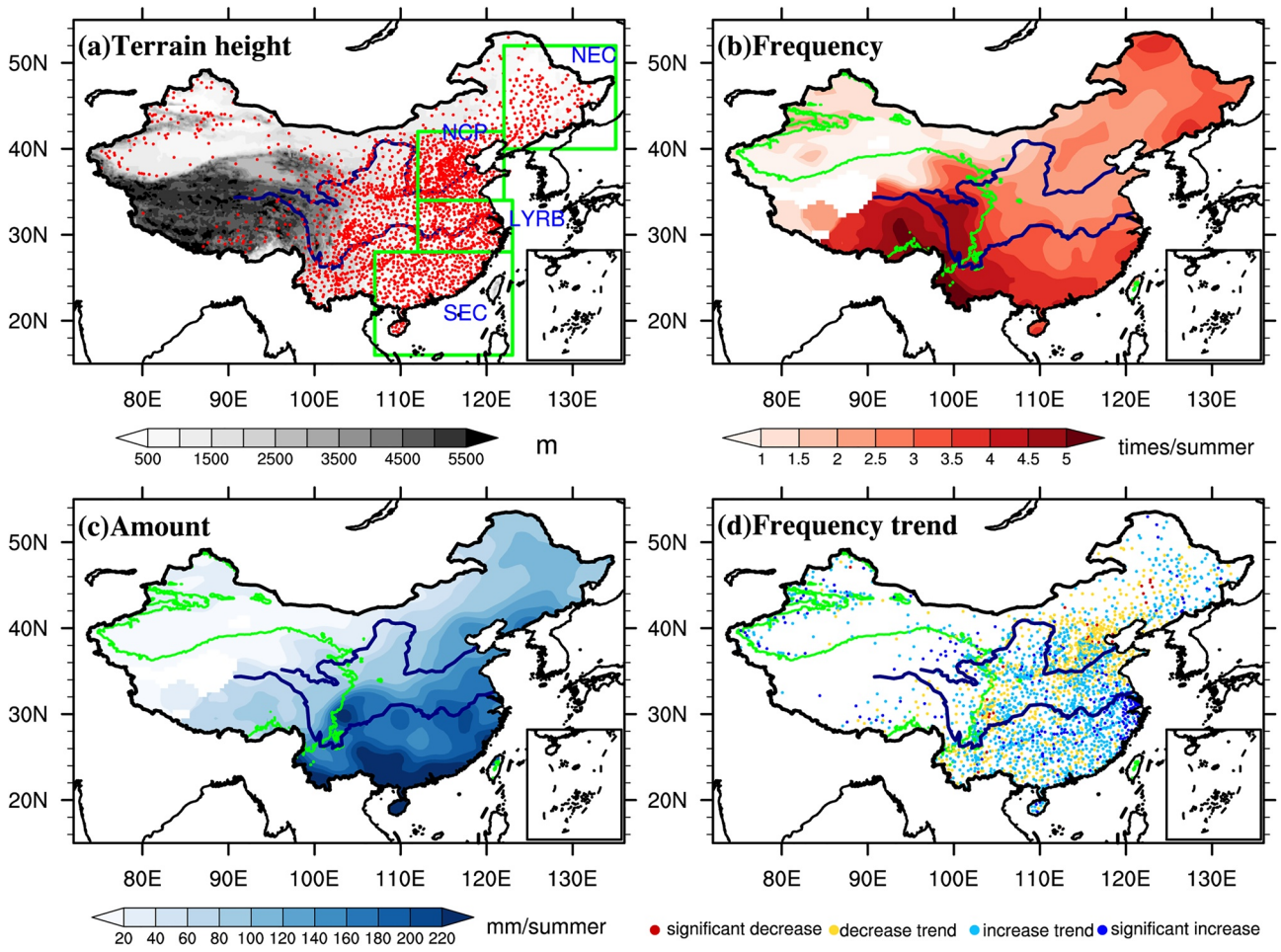

Figure 1. Spatiotemporal characteristics of summer extreme precipitation in China. Station distribution (red dots) and sub-region boundaries (green boxes) are shown in (a) (southeastern China [SEC]: 107°–123°E, 16°N–28°N, the Lower reach of the Yangtze River Basin (LYRB): 112°–123°E, 28°–34°N, North China Plain (NCP): 112°–122°E, 34°–42°N, northeastern China (NEC): 122°–135°E, 40°–52°N), with the surface terrain height shaded. Average extreme precipitation frequency and amount are shown in (b) and (c), linear regression trends of extreme precipitation frequency at stations are shown in (d), the statistical significance is tested by Student-t test and significant level of 0.05 is selected. The green lines in (b) to (d) are the contour of 2500 m height.

about 53% to the total REPE, the southwesterly of the vortex prevails in the southwestern part where relative higher EP occurrence probability occurs (Figure 2g). The monsoon-like pattern 2 is characterized by prevailing southwesterly (northwesterly) over south (north) of northeastern China, under which EP tends to occur in the southwest (Figure 2h). Around 40% cases of the cyclone-like pattern 3 (Figure 2i) are contributed by the landfalling TCs (Figure 3d), the other cases can be low vortexes shifting eastward, and EP is likely to happen in the southeast of northeastern China under this pattern. Over North China Plain, the two synoptic patterns are dominated by low-level southwesterly and southeasterly, respectively (Figures 2j and 2k). Most cases of REPE (~82%) happen under the synoptic pattern 1 with relative smaller EP occurrence probability spread over the region. Pattern 2 only leads to around 18% cases of total REPE, but much higher occurrence probability of EP is noted in the west and north of North China Plain under this pattern compared to pattern 1.

Generally, the synoptic patterns characterized by EASM and the Meiyu front contributes about 70% (P1), 90% (P1 + P2), and 80% (P1) to the total REPE over southeastern China, the Lower reach of the Yangtze River Basin, and North China Plain, respectively. For the landfalling TCs, they have contributed to the REPE over southeastern China and the Lower reach of the Yangtze River Basin by ~30% and ~8.2%, respectively. Because only about 40% cases of pattern 3 over northeastern China are contributed by the landfalling TCs and the other cases can be related to low vortexes, we can say that about 60% of REPE over northeastern China are resulted from the low vortexes, while the summer monsoon and landfalling TCs contribute approximately 35% and 5%, respectively.

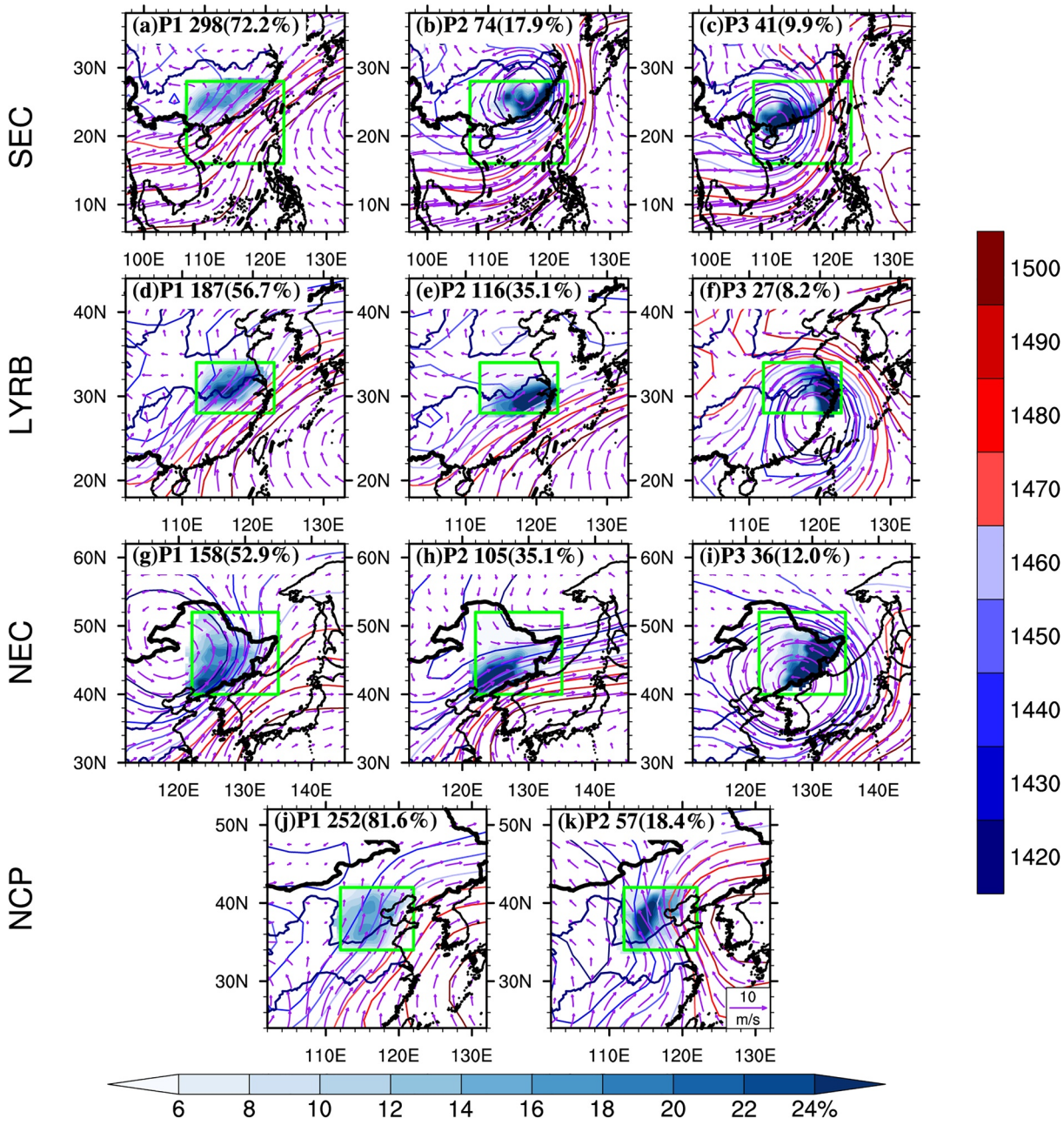

Figure 2. The synoptic patterns responsible for regional extreme precipitation events (REPE) over each sub-region of East China revealed by clustering at 850 hPa. The average fields of each synoptic pattern are shown. Each row shows different patterns over a sub-region, filled value (bottom color bar) is the occurrence probability of extreme precipitation (see text), vectors refer to winds and contours refer to geopotential heights (right color bar, units: gpm). Pattern name ("P1" means pattern 1), total occurrence and proportion of each synoptic pattern to the total occurrence of REPE are shown in the subtitle.

3.3. Joint Actions of Multiple Systems

The positions of WNPSH, SAH, and EASJ play important roles in the formation of summer EP over East China (Ge et al., 2019; Ning et al., 2017; Yokoyama et al., 2017; Q. Zhang et al., 2017). To examine how the different synoptic patterns affect the REPE over each sub-region, Figure 4 further gives the configurations of these multi-level systems under different synoptic patterns.

Under the monsoon-like patterns (Figures 4a, 4d, 4e, 4h, 4j, and 4k), SAH tends to extend eastward and northward compared to summer climatological position (except for pattern 1 over southeastern China), and

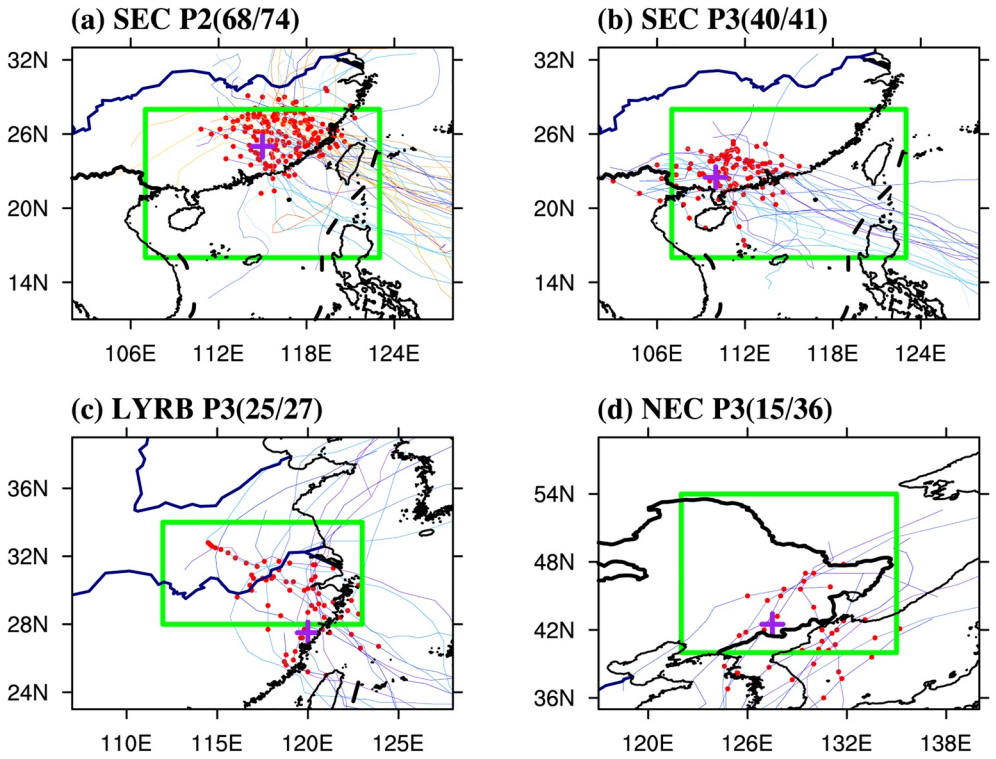

Figure 3. Contributions of tropical cyclones (TCs) to cyclone-like patterns. Lines with different colors indicate the paths of different TCs, red dots show the locations of tropical cyclone centers during regional extreme precipitation events (REPE), purple cross indicates the location of the cyclone center (defined as grid with smaller geopotential height than the eight grid points around) at the 850 hPa average field of a given cyclone-like pattern. Green boxes are the region boundaries. Only TCs with the centers close enough to the cyclone center (within 5° around) during REPE are selected (in other words, TCs with path drown all have at least one red point close enough to the purple cross). TC record number and total cases of the cyclone-like patterns are shown in the subtitle. Pattern 1 over northeastern China is not considered because there are only two records of TCs close enough within the 158 cases in total.

EASJ shifts southward in the southern two sub-regions and northward in the northern two sub-regions, while WNPSH tends to extend northwestward except for pattern 2 of North China Plain. The northwestward extension of WNPSH leads to significant positive anomaly of geopotential height and strong southwest water vapor transport, which finally leads to higher EP occurrence probability combined with the strong updrafts at 700 hPa. The two synoptic patterns over North China Plain show some differences, they are characterized by an anomalous high around Korean at 850 hPa, and the water vapor paths are different, it comes from South China Sea under pattern 1 and East China Sea as well as Yellow Sea under pattern 2, respectively. Obviously, higher EP occurrence probability is likely to occur at northeast of SAH, south of EASJ and northwest of WNPSH under monsoon-like patterns.

Under the cyclone-like patterns (Figures 4b, 4c, 4f, 4g, and 4i), the SAH tends to extend farther northeast, which favors the formation of upper-level divergence, the EASJ all shifts northward correspondingly. While the WNPSH can affect the moving path of landfalling TCs, for example, under pattern 2 (3) over southeastern China the farther east (west) location of WNPSH guides the TCs turning northward (moving northwestward) (Figures 3a and 3b). The eastward retreat of WNPSH is favorable for the eastward movement of vortexes under patterns 1 and 3 over northeastern China. Overall, the water vapor transport from South China Sea and East China Sea driven by the cyclones including landfalling TCs leads to high EP occurrence probability with the cooperation of strong updrafts.

It can be noted that the coverage of large positive divergence of 200 hPa anomalous winds over the northeast of SAH and south of EASJ matches well with the locations of strong updrafts and high EP occurrence probability, indicating the SAH and EASJ play important roles in the formation of strong updrafts via

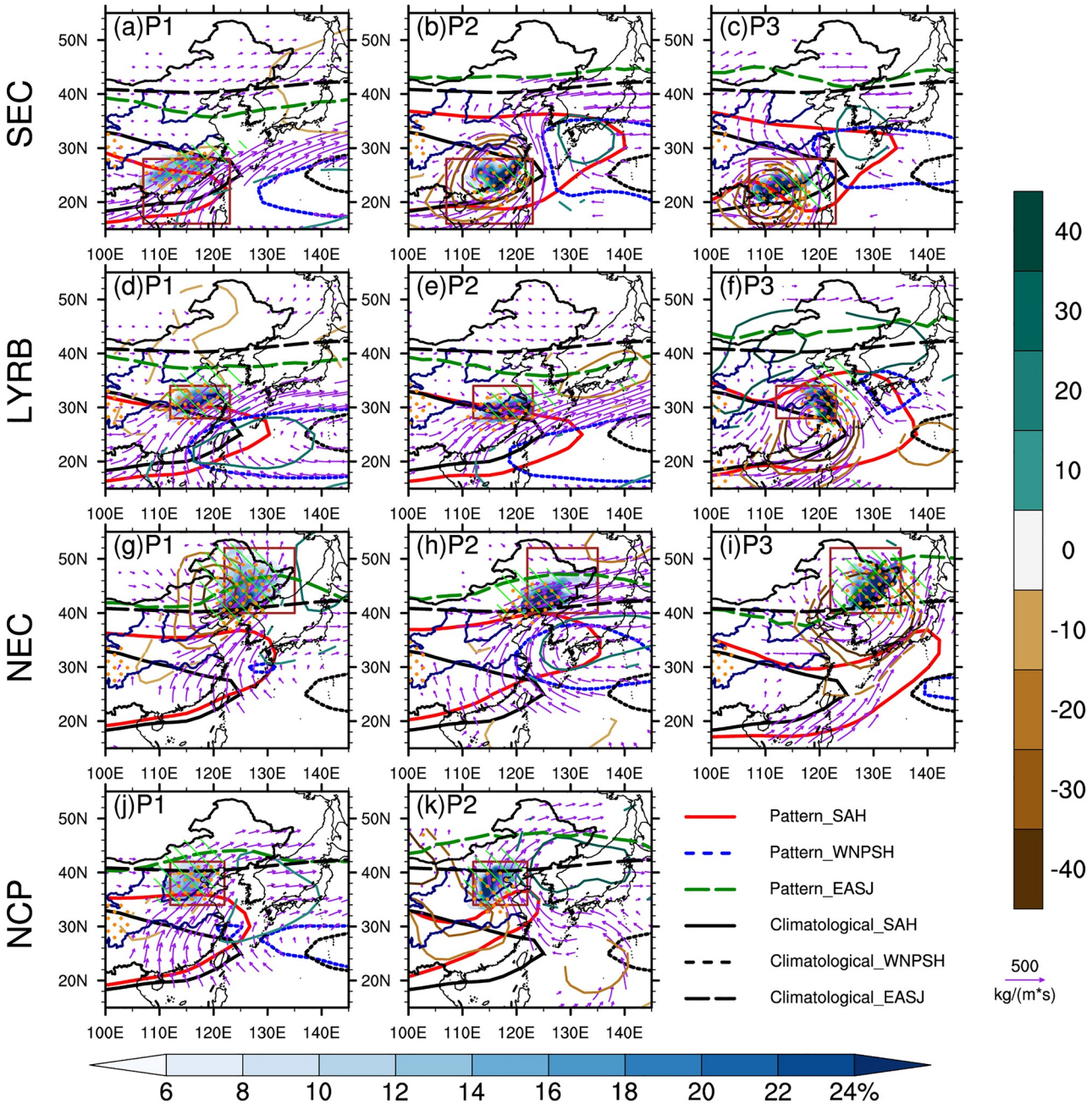

Figure 4. Configuration of South Asian High (SAH), western North Pacific subtropical high (WNPSH), and Eastern Asian Subtropical Jet (EASJ) under each synoptic pattern. Solid lines refer to SAH, short dashed lines refer to WNPSH, and long dashed lines refer to the axis of EASJ. Red, blue, and green lines show the position of SAH, WNPSH, and EASJ under each synoptic pattern, respectively. The black lines show their summer climatological positions. Vectors indicate the vertically integrated water vapor flux (1000–300 hPa) which is significant. Thicker contour lines indicate the significant geopotential height (gpm) under each synoptic pattern, all significant level is 0.05 tested by Student-t test. Green slashes indicate that the anomalous wind divergence at 200 hPa is more than 4×10^{-6} s^{-1}. Orange dotted areas indicate the ascent speed is more than 1 cm s^{-1} at 700 hPa. Shaded values are the occurrence probability of extreme precipitation like Figure 2.

divergence pumping effect (B. Liu et al., 2015; Yokoyama et al., 2017). In all, the REPE over East China are results of joint action of multi-level systems, the WNPSH and cyclones including landfalling TCs drive the water vapor transport, while SAH and EASJ are favorable for the strong updrafts. Different configurations of multiple systems determine the distributions of EP occurrence probability under different patterns.

3.4. Long-Term Trends

The monsoon-like synoptic patterns over southeastern China and the Lower reach of the Yangtze River Basin mainly appear in June and their occurrences show increasing trend during the past 6 decades (Figures 5a, 5d, and 5e). The monsoon-like pattern 2 over northeastern China shows a slight increasing trend and concentrates in July and August, in accordance with the period when the monsoon-like background circulation is likely to occur (Zhao et al., 2018) (Figure 5h). The two synoptic patterns over North China Plain mostly occur in mid-to-late summer with the occurrences of pattern 1 (2) showing an insignificant increasing (a significant decreasing) trend (Figures 5j and 5k). It can be seen that most monsoon-like patterns (pattern 1 over southeastern China and the Lower reach of the Yangtze River Basin, pattern 2 over northeastern China and North China Plain) decreased from 1960s to 1990s, abruptly increased during 1990s and reduced after 2000, corresponding to the weakening and recovery of EASM (Ding et al., 2008; Han et al., 2015; H. Liu et al., 2012; Xu et al., 2006).

All cyclone-like patterns show increasing trends during the past 6 decades and most of them occur in July and August (Figures 5b, 5c, 5f, 5g, and 5i). The increasing occurrences of these patterns are consistent with the increasing frequency and intensity of TCs over northwestern Pacific (Kossin et al., 2020; Mei & Xie, 2016; Qiu et al., 2019). Over southeastern China, the synoptic pattern 2 shows a slight increasing trend (Figure 5b), while pattern 3 occurs more frequently since 1996 (Figure 5c). Over the Lower reach of the Yangtze River Basin, pattern 3 occurs more frequently since 1986, and a significant increasing trend can be detected (Figure 5f). Over northeastern China, pattern 1 characterized by the low-level vortex distributes evenly and displays a weak increasing trend. Synoptic pattern 3 characterized by a mixture of vortices shifting southeastward (~60%) and landfalling TCs (~40%) shows decadal changes with relative higher occurrences in 1960s, 1980s, and 2010s to some extent (Figure 5i).

The changing rates of REPE occurrences ranging from −0.09 to 0.87 times decade^{-1} over East China exhibit regional differences, with the fastest increasing trend over the Lower reach of the Yangtze River Basin and a slight decreasing trend over North China Plain (Figure 5l). Both the monsoon-like pattern (pattern 1) and cyclone-like patterns (patterns 2 and 3) with comparable increasing trend (0.22 vs. 0.19 times decade^{-1}) result in the total increasing trend of REPE occurrences over southeastern China. The significant increasing trend of REPE occurrences over the Lower reach of the Yangtze River Basin is largely determined by the monsoon-like patterns (patterns 1 and 2) with the intensity of ~78% Meanwhile, the occurrences of pattern 2 characterized by the Meiyu front and the cyclone-like pattern 3 characterized by landfalling TCs increase significantly by 0.49 and 0.19 times decade^{-1}, respectively. The slight decreasing trend of REPE occurrences over the North China Plain is mainly resulted from the significantly reduced synoptic pattern 2, which offsets the increase of the synoptic pattern 1. All three synoptic patterns over northeastern China consistently show increasing trends, with pattern 2 exhibiting the fastest increase rate. In addition to the primary contribution of monsoon-like pattern, the increase of landfalling TCs (0.03 times decade^{-1}) leads to the secondary contribution to the increasing trend of the REPE occurrences over northeastern China.

4. Summary and Discussion

Toward risk assessment and climate prediction of EP events, this paper has explored the potential of an indirect method: links between synoptic weather patterns and summer EP. Based on this principle, synoptic patterns associated with summer REPE over each sub-region of East China have been detected by spectral clustering systematically and quantitatively. Weather systems responsible for regional events, as well as their contribution to the occurrences and variations of REPE are investigated. Synoptic patterns related to EASM and TCs are responsible for about 70% of regional events over East China. Meanwhile, the Meiyu front and low-level vortex also have considerable contributions to the REPE over the Lower reach of the Yangtze River Basin and northeastern China, respectively.

Most sub-regions show increasing trends of REPE during the past 6 decades. Over southeastern China, the monsoon-like and cyclone-like synoptic patterns have comparable contributions to the increase of REPE, while the synoptic pattern characterized by the Meiyu front dominates the robust increasing REPE over the Lower reach of the Yangtze River Basin. Long-term decrease of synoptic pattern characterized by low-level

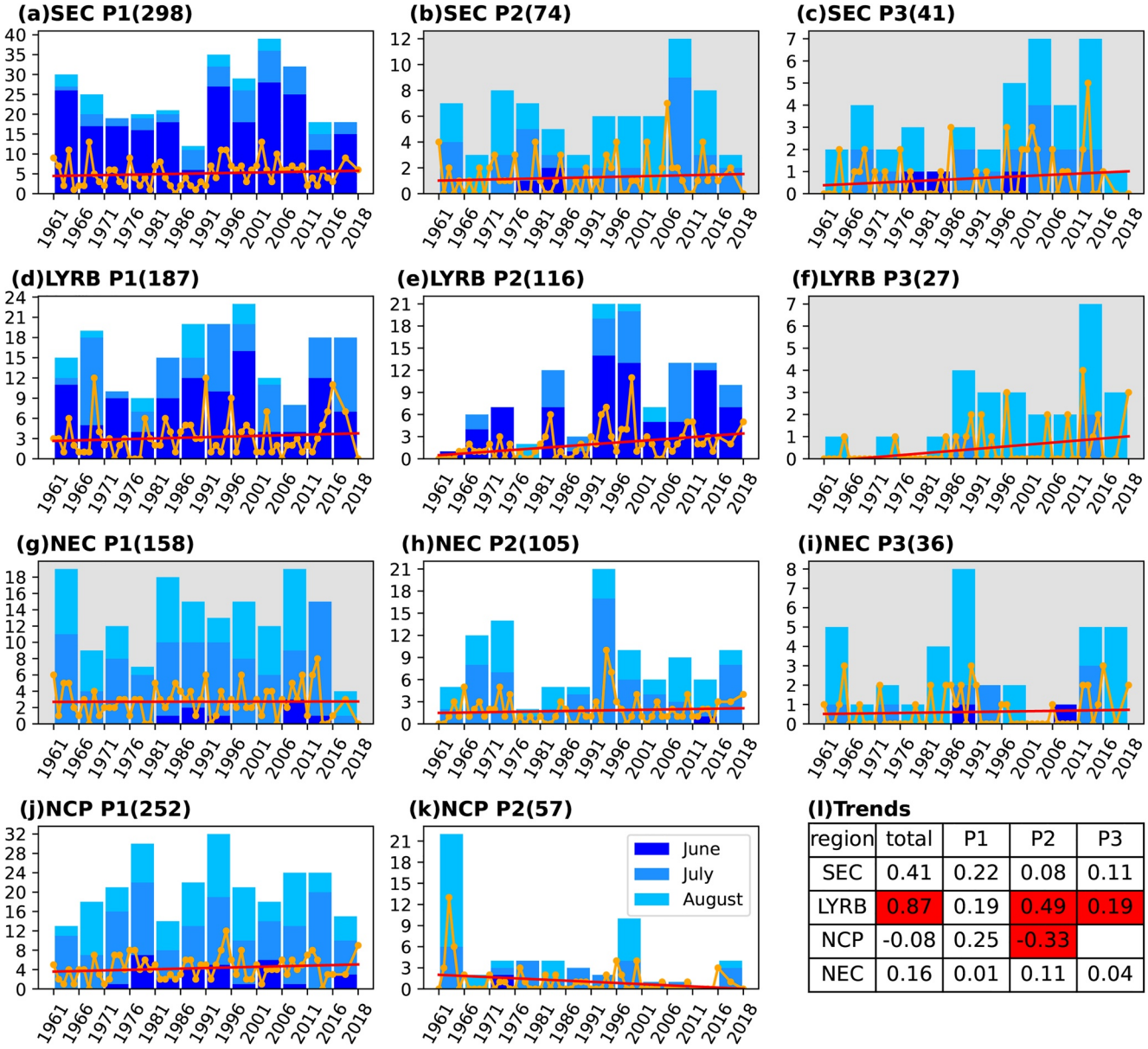

(l)Trends

region	total	P1	P2	P3
SEC	0.41	0.22	0.08	0.11
LYRB	0.87	0.19	0.49	0.19
NCP	-0.08	0.25	-0.33	
NEC	0.16	0.01	0.11	0.04

Figure 5. Temporal variations of synoptic patterns associated with the regional extreme precipitation events (REPE) over eastern China. Stacked histograms (a–k) show the occurrences of synoptic patterns every 5 years (except for the last bar which shows the occurrences of 3 years from 2016 to 2018), different colors indicate the occurrences in different months. Orange lines show the occurrences of the patterns in each summer and red lines are linear regression lines. Sub-region name and synoptic pattern name are shown in the subtitle, followed by the total occurrence of the pattern in the bracket. Cyclone-like patterns are emphasized by light-gray background. Linear trends of total REPE and each pattern are shown in (l) (units: times/decade), with significant (0.05 level) trends indicated by red backgrounds.

southeasterly over the North China Plain is responsible for the significant decrease of REPE there. Over northeastern China, the monsoon-like pattern dominates the increase of REPE.

Extremes are, by definition, low-probability high impact events. It remains a challenge to predict the occurrence, intensity, and location of a particular extreme event. Predicting EP is even more challenging because of the crude representation of rainfall processes in numerical models and the limitation of current model resolutions. Some researchers have introduced the weather-pattern-based methods on precipitation prediction, and infer that the methods are more skillful in heavy rain prediction than traditional methods (Gottardi et al., 2012; Nguyen-Le et al., 2017; Nguyen-Le & Yamada, 2019; Vuillaume & Herath, 2017). This study demonstrates a novel approach in identifying synoptic drivers of EP events. The results will enable us

to develop indirect methods for predicting extreme rainfall events and risk assessment of future extremes under a growing global warming trend.

Limited by the lack of long-term and fine resolution data, we can only apply clustering on 2.5° reanalysis data at present. A comparison with the results using the latest ERA5 data clustered by the same method and the results using NCEP data after 1979 (not shown) shows slight difference from our conclusions.

Data Availability Statement

The authors are also grateful to CMA (http://tcdata.typhoon.org.cn/), NCEP (https://psl.noaa.gov/data/gridded/data.ncep.reanalysis.pressure.html), and ECMWF (https://www.ecmwf.int/en/forecasts/datasets/reanalysis-datasets/era5) for allowing them to use the data.

Acknowledgments
This work was supported by the National Key R&D Program of China under grant 2016YFA0602104 and the National Natural Science Foundation of China under grants 41975081. Danqing Huang acknowledges the founding support from the National Key R&D Program of China (Grant 2016YFA0600701) and the National Natural Science Foundation of China (Grants 41930969 and 42075020). Peili Wu was funded by the UK–China Research Innovation Partnership Fund through the Met Office Climate Science for Service Partnership (CSSP) China as part of the Newton Fund. Anning Huang acknowledges the CAS "Light of West China" Program, and the Jiangsu University "Blue Project" outstanding young teachers training object, the Fundamental Research Funds for the Central Universities and the Jiangsu Collaborative Innovation Center for Climate Change. The authors appreciate the two anonymous reviewers for their constructive and insightful suggestions to greatly help improve the manuscript.

References

Amini, S., & Straus, D. M. (2019). Control of storminess over the Pacific and North America by circulation regimes. *Climate Dynamics*, *52*(7), 4749–4770. https://doi.org/10.1007/s00382-018-4409-7

Beniston, M., Stephenson, D. B., Christensen, O. B., Ferro, C. A. T., Frei, C., Goyette, S., et al. (2007). Future extreme events in European climate: An exploration of regional climate model projections. *Climatic Change*, *81*(1), 71–95. https://doi.org/10.1007/s10584-006-9226-z

Caliński, T., & Harabasz, J. (1974). A dendrite method for cluster analysis. *Communication in Statistics – Theory and Methods*, *3*(1), 1–27. https://doi.org/10.1080/03610927408827101

Chen, H. (2013). Projected change in extreme rainfall events in China by the end of the 21st century using CMIP5 models. *Chinese Science Bulletin*, *58*(12), 1462–1472. https://doi.org/10.1007/s11434-012-5612-2

Chen, Y., & Zhai, P. (2014). Precursor circulation features for persistent extreme precipitation in Central-Eastern China, *Weather Forecasting*, *29*(2), 226–240. https://doi.org/10.1175/waf-d-13-00065.1

Ding, Y., Wang, Z., & Sun, Y. (2008). Inter-decadal variation of the summer precipitation in East China and its association with decreasing Asian summer monsoon. Part I: Observed evidences. *International Journal of Climatology*, *28*(9), 1139–1161. https://doi.org/10.1002/joc.1615

Donat, M. G., Lowry, A. L., Alexander, L. V., O'Gorman, P. A., & Maher, N. (2016). More extreme precipitation in the world's dry and wet regions. *Nature Climate Change*, *6*(5), 508–513. https://doi.org/10.1038/nclimate2941

Dong, Q., Chen, X., & Chen, T. (2011). Characteristics and changes of extreme precipitation in the Yellow–Huaihe and Yangtze–Huaihe Rivers Basins, China. *Journal of Climate*, *24*(14), 3781–3795. https://doi.org/10.1175/2010jcli3653.1

Fereday, D. R., Knight, J. R., Scaife, A. A., Folland, C. K., & Philipp, A. (2008). Cluster analysis of North Atlantic–European circulation types and links with tropical Pacific Sea surface temperatures. *Journal of Climate*, *21*(15), 3687–3703. https://doi.org/10.1175/2007jcli1875.1

Ge, J., You, Q., & Zhang, Y. (2019). Effect of Tibetan Plateau heating on summer extreme precipitation in eastern China. *Atmospheric Research*, *218*, 364–371. https://doi.org/10.1016/j.atmosres.2018.12.018

Gottardi, F., Obled, C., Gailhard, J., & Paquet, E. (2012). Statistical reanalysis of precipitation fields based on ground network data and weather patterns: Application over French mountains. *Journal of Hydrology*, *432–433*, 154–167. https://doi.org/10.1016/j.jhydrol.2012.02.014

Han, T., Chen, H., & Wang, H. (2015). Recent changes in summer precipitation in Northeast China and the background circulation. *International Journal of Climatology*, *35*(14), 4210–4219. https://doi.org/10.1002/joc.4280

Horton, D. E., Johnson, N. C., Singh, D., Swain, D. L., Rajaratnam, B., & Diffenbaugh, N. S. (2015). Contribution of changes in atmospheric circulation patterns to extreme temperature trends. *Nature*, *522*(7557), 465–469. https://doi.org/10.1038/nature14550

Houssos, E. E., Lolis, C. J., & Bartzokas, A. (2008). Atmospheric circulation patterns associated with extreme precipitation amounts in Greece. *Advances in Geosciences*, *17*, 5–11. https://doi.org/10.5194/adgeo-17-5-2008

Hu, Y., Deng, Y., Zhou, Z., Cui, C., & Dong, X. (2019). A statistical and dynamical characterization of large-scale circulation patterns associated with summer extreme precipitation over the middle reaches of Yangtze River. *Climate Dynamics*, *52*(9), 6213–6228. https://doi.org/10.1007/s00382-018-4501-z

Huang, D.-Q., Zhu, J., Zhang, Y.-C., & Huang, A.-N. (2014). The different configurations of the East Asian polar front jet and subtropical jet and the associated rainfall anomalies over Eastern China in summer. *Journal of Climate*, *27*(21), 8205–8220. https://doi.org/10.1175/jcli-d-14-00067.1

Keller, S., & Atzl, A. (2014). Mapping natural hazard impacts on road infrastructure—The extreme precipitation in Baden-Württemberg, Germany, June 2013. *International Journal of Disaster Risk Science*, *5*(3), 227–241. https://doi.org/10.1007/s13753-014-0026-1

Kharin, V. V., Zwiers, F. W., Zhang, X., & Wehner, M. (2013). Changes in temperature and precipitation extremes in the CMIP5 ensemble. *Climatic Change*, *119*(2), 345–357. https://doi.org/10.1007/s10584-013-0705-8

Kossin, J. P., Knapp, K. R., Olander, T. L., & Velden, C. S. (2020). Global increase in major tropical cyclone exceedance probability over the past four decades. *Proceedings of National Academy of Sciences of the United States of America*, *117*(22), 11975–11980. https://doi.org/10.1073/pnas.1920849117

Li, L., & Zhang, Y. (2014). Effects of different configurations of the East Asian subtropical and polar front jets on precipitation during the Mei-Yu season. *Journal of Climate*, *27*(17), 6660–6672. https://doi.org/10.1175/jcli-d-14-00021.1

Li, R. C. Y., & Zhou, W. (2015). Interdecadal changes in summertime tropical cyclone precipitation over Southeast China during 1960–2009. *Journal of Climate*, *28*(4), 1494–1509. https://doi.org/10.1175/jcli-d-14-00246.1

Liu, B., Wu, G., & Ren, R. (2015). Influences of ENSO on the vertical coupling of atmospheric circulation during the onset of South Asian summer monsoon. *Climate Dynamics*, *45*(7), 1859–1875. https://doi.org/10.1007/s00382-014-2439-3

Liu, H., Zhou, T., Zhu, Y., & Lin, Y. (2012). The strengthening East Asia summer monsoon since the early 1990s. *Chinese Science Bulletin*, *57*(13), 1553–1558. https://doi.org/10.1007/s11434-012-4991-8

Luo, Y., Wu, M., Ren, F., Li, J., & Wong, W.-K. (2016). Synoptic situations of extreme hourly precipitation over China. *Journal of Climate*, *29*(24), 8703–8719. https://doi.org/10.1175/jcli-d-16-0057.1

Mei, W., & Xie, S.-P. (2016). Intensification of landfalling typhoons over the northwest Pacific since the late 1970s. *Nature Geoscience*, *9*(10), 753–757. https://doi.org/10.1038/ngeo2792

Nguyen-Le, D., & Yamada, T. J. (2019). Using weather pattern recognition to classify and predict summertime heavy rainfall occurrence over the upper Nan River Basin, Northwestern Thailand, *Weather Forecasting*, *34*(2), 345–360. https://doi.org/10.1175/waf-d-18-0122.1

Nguyen-Le, D., Yamada, T. J., & Tran-Anh, D. (2017). Classification and forecast of heavy rainfall in northern Kyushu during Baiu season using weather pattern recognition. *Atmospheric Science Letters*, *18*(8), 324–329. https://doi.org/10.1002/asl.759

Ning, L., Liu, J., & Wang, B. (2017). How does the South Asian high influence extreme precipitation over eastern China? *Journal of Geophysical Research*, *122*(8), 4281–4298. https://doi.org/10.1002/2016jd026075

Ohba, M., & Sugimoto, S. (2019). Differences in climate change impacts between weather patterns: Possible effects on spatial heterogeneous changes in future extreme rainfall. *Climate Dynamics*, *52*(7), 4177–4191. https://doi.org/10.1007/s00382-018-4374-1

Pedregosa, F., Varoquaux, G., Gramfort, A., Michel, V., Thirion, B., Grisel, O., et al. (2011). Scikit-learn: Machine learning in Python. *Journal of Machine Learning Research*, *12*(85), 2825–2830.

Pfahl, S., O'Gorman, P. A., & Fischer, E. M. (2017). Understanding the regional pattern of projected future changes in extreme precipitation. *Nature Climate Change*, *7*(6), 423–427. https://doi.org/10.1038/nclimate3287

Qiu, W., Ren, F., Wu, L., Chen, L., & Ding, C. (2019). Characteristics of tropical cyclone extreme precipitation and its preliminary causes in Southeast China. *Meteorology and Atmospheric Physics*, *131*(3), 613–626. https://doi.org/10.1007/s00703-018-0594-5

Riddle, E. E., Stoner, M. B., Johnson, N. C., L'Heureux, M. L., Collins, D. C., & Feldstein, S. B. (2013). The impact of the MJO on clusters of wintertime circulation anomalies over the North American region. *Climate Dynamics*, *40*(7), 1749–1766. https://doi.org/10.1007/s00382-012-1493-y

Rosenberg, E. A., Keys, P. W., Booth, D. B., Hartley, D., Burkey, J., Steinemann, A. C., & Lettenmaier, D. P. (2010). Precipitation extremes and the impacts of climate change on stormwater infrastructure in Washington State, *Climatic Change*, *102*(1), 319–349. https://doi.org/10.1007/s10584-010-9847-0

Rosenzweig, C., Tubiello, F. N., Goldberg, R., Mills, E., & Bloomfield, J. (2002). Increased crop damage in the US from excess precipitation under climate change. *Global Environmental Changes – -Human and Policy Dimensions*, *12*(3), 197–202. https://doi.org/10.1016/s0959-3780(02)00008-0

Schlef, K. E., Moradkhani, H., & Lall, U. (2019). Atmospheric circulation patterns associated with extreme United States floods identified via machine learning. *Scientific Reports*, *9*(1), 7171. https://doi.org/10.1038/s41598-019-43496-w

Stahl, K., Moore, R. D., & Mckendry, I. G. (2006). The role of synoptic-scale circulation in the linkage between large-scale ocean–atmosphere indices and winter surface climate in British Columbia, Canada. *International Journal of Climatology*, *26*(4), 541–560. https://doi.org/10.1002/joc.1268

Su, B. D., Jiang, T., & Jin, W. B. (2006). Recent trends in observed temperature and precipitation extremes in the Yangtze River basin, China, *Theoretical and Applied Climatology*, *83*(1), 139–151. https://doi.org/10.1007/s00704-005-0139-y

Swales, D., Alexander, M., & Hughes, M. (2016). Examining moisture pathways and extreme precipitation in the U.S. Intermountain West using self-organizing maps. *Geophysical Research Letters*, *43*(4), 1727–1735. https://doi.org/10.1002/2015gl067478

Tebaldi, C., Hayhoe, K., Arblaster, J. M., & Meehl, G. A. (2006). Going to the extremes. *Climatic Changes*, *79*(3), 185–211. https://doi.org/10.1007/s10584-006-9051-4

Utsumi, N., Kim, H., Kanae, S., & Oki, T. (2016). Which weather systems are projected to cause future changes in mean and extreme precipitation in CMIP5 simulations? *Journal of Geophysical Research*, *121*(18), 10522–510537. https://doi.org/10.1002/2016jd024939

Utsumi, N., Kim, H., Kanae, S., & Oki, T. (2017). Relative contributions of weather systems to mean and extreme global precipitation. *Journal of Geophysical Research*, *122*(1), 152–167. https://doi.org/10.1002/2016jd025222

van Oldenborgh, G. J., van der Wiel, K., Sebastian, A., Singh, R., Arrighi, J., Otto, F., et al. (2017). Attribution of extreme rainfall from Hurricane Harvey. *Environmental Research Letters*, *12*(12). 124009. https://doi.org/10.1088/1748-9326/aa9ef2

Vogel, E., Donat, M. G., Alexander, L. V., Meinshausen, M., Ray, D. K., Karoly, D., et al. (2019). The effects of climate extremes on global agricultural yields. *Environmental Research Letters*, *14*(5), 054010. https://doi.org/10.1088/1748-9326/ab154b

von Luxburg, U. (2007). A tutorial on spectral clustering. *Statistics and Computing*, *17*(4), 395–416. https://doi.org/10.1007/s11222-007-9033-z

Vuillaume, J.-F., & Herath, S. (2017). Improving global rainfall forecasting with a weather type approach in Japan. *Hydrological Sciences Journal*, *62*(2), 167–181. https://doi.org/10.1080/02626667.2016.1183165

Wang, Y., & Zhou, L. (2005). Observed trends in extreme precipitation events in China during 1961–2001 and the associated changes in large-scale circulation. *Geophysical Research Letters*, *32*(9), L17708. https://doi.org/10.1029/2005gl023769

Wu, H., Zhai, P., & Chen, Y. (2016). A comprehensive classification of anomalous circulation patterns responsible for persistent precipitation extremes in South China. *Journal of Meteorological Research*, *30*(4), 483–495. https://doi.org/10.1007/s13351-016-6008-z

Xiao, C., Wu, P., Zhang, L., & Song, L. (2016). Robust increase in extreme summer rainfall intensity during the past four decades observed in China. *Scientific Reports*, *6*, 38506. https://doi.org/10.1038/srep38506

Xie, Z., Du, Y., Zeng, Y., & Miao, Q. (2018). Classification of yearly extreme precipitation events and associated flood risk in the Yangtze-Huaihe River Valley. *Science China Earth Sciences*, *61*(9), 1341–1356. https://doi.org/10.1007/s11430-017-9212-8

Xu, M., Chang, C.-P., Fu, C., Qi, Y., Robock, A., Robinson, D., & Zhang, H.-m. (2006). Steady decline of east Asian monsoon winds, 1969–2000: Evidence from direct ground measurements of wind speed. *Journal of Geophysical Research*, *111*(D24), D24111. https://doi.org/10.1029/2006jd007337

Yao, C., Qian, W., Yang, S., & Lin, Z. (2010). Regional features of precipitation over Asia and summer extreme precipitation over Southeast Asia and their associations with atmospheric–oceanic conditions. *Meteorology and Atmospheric Physics*, *106*(1), 57–73. https://doi.org/10.1007/s00703-009-0052-5

Ying, M., Zhang, W., Yu, H., Lu, X., Feng, J., Fan, Y., et al. (2014). An overview of the China meteorological administration tropical cyclone database. *Journal of Atmospheric and Oceanic Technology*, *31*(2), 287–301. https://doi.org/10.1175/jtech-d-12-00119.1

Yokoyama, C., Takayabu, Y. N., & Horinouchi, T. (2017). Precipitation characteristics over East Asia in early summer: Effects of the subtropical jet and lower-tropospheric convective instability. *Journal of Climate*, *30*(20), 8127–8147. https://doi.org/10.1175/jcli-d-16-0724.1

Zhang, C., Zhang, Q., Wang, Y., & Liang, X. (2008). Climatology of warm season cold vortices in East Asia: 1979–2005. *Meteorology and Atmospheric Physics*, *100*(1), 291–301. https://doi.org/10.1007/s00703-008-0310-y

Zhang, H., & Zhai, P. (2011). Temporal and spatial characteristics of extreme hourly precipitation over eastern China in the warm season. *Advances in Atmospheric Sciences*, *28*(5), 1177–1183. https://doi.org/10.1007/s00376-011-0020-0

Zhang, Q., Zheng, Y., Singh, V. P., Luo, M., & Xie, Z. (2017). Summer extreme precipitation in eastern China: Mechanisms and impacts. *Journal of Geophysical Research*, *122*(5), 2766–2778. https://doi.org/10.1002/2016jd025913

Zhang, X., Zwiers, F. W., Li, G., Wan, H., and Cannon, A. J. (2017). Complexity in estimating past and future extreme short-duration rainfall. *Nat. Geosci.*, *10*(4), 255–259.

Zhao, J., Zhou, J., Yang, L., Hou, W., & Feng, G. (2018). Inter-annual and inter-decadal variability of early- and late-summer precipitation over northeast China and their background circulation. *International Journal of Climatology*, *38*(6), 2880–2888. https://doi.org/10.1002/joc.5470

Zheng, Y., Chen, J., Ge, G., & Zhu, P. (2008). Typical structure, variety, and multi-scale characteristics of Meiyu front. *Journal of Meteorological Research*, *22*(2), 187–201.